Fault Diagnosis Of New Energy Vehicle System Based On Deep Learning

Zhengqian Wu*

Hunan Mechanical & Electrical Polytechnic, Changsha,410151 China

* *Corresponding author. E-mail: zhengqianwu008@outlook.com*

Received: May. 05, 2026; Accepted: Jun. 26, 2026

New energy vehicles (NEVs), powered by sustainable energy, are emerging as a cleaner alternative to conventional vehicles. Their performance and safety depend heavily on the health of critical components, making accurate fault diagnosis essential. This study proposes an advanced fault detection framework for NEVs, focusing on fault identification and classification in the drivetrain using deep learning techniques. Sensor data from electric vehicles, including current, voltage, motor speed, and environmental conditions, are pre-processed through normalization and missing-value imputation to ensure consistency. Feature extraction is performed using Wavelet Transform (WT) and Fast Fourier Transform (FFT) to capture both transient and steady-state behaviours. The proposed Enriched Crow Search Optimizer-based Adaptive Gated Long Short-Term Memory (ECS-AG-LSTM) model enhances LSTM adaptability and fault classification accuracy through optimization. Experimental results demonstrate superior performance, achieving 98.5% accuracy, 98.31% recall, 98.42% precision, 98.51% F1-score, and an R^2 value of 0.956 . The findings confirm that ECS-AG-LSTM provides a robust and reliable solution for improving NEV safety and operational dependability.

Keywords: New Energy Vehicles (NEVs), Fault Diagnosis, Deep Learning (DL), Enriched Crow Search Optimizer-driven Adaptive Gated Long Short-Term Memory (ECS-AGLSTM), Sensor Data ion.

http://dx.doi.org/10.6180/jase.202611_34.034

1. Introduction

Depend on correct diagnosis of faults in complex drivetrain systems to ensure the reliability, safety and efficiency of the NEV. Even if the NEVs contribute to sustainable transportation with less environmental burden [1]. NEV system is composed of connected components, and the fault be caused by failure of sensor, damage of motor winding, malfunction of inverter [2]. Efficient fault diagnosis improves safety, reliability, consumer confidence, and NEV adoption. [3] FDD techniques promote early defect detection and prediction of maintenance for electric motors [4]. Electric motors are a component of NEV powertrains and are built upon mechanical and electrical subsystems [5]. Voltage faults point to an internal device being damaged; monitoring the voltage detect latent failures of the battery [6]. The proposed ECS-AG-LSTM model is capable of distinguishing the accurate fault type of the NEV drivetrain.

NEVs are promising such that they are less polluting and more energy efficient than traditional vehicles. Their drivetrain architecture is composed of various interacting subsystems, namely batteries, motors, inverters and sensors, all of which contribute to the seamless operation of the vehicle. Faults in any of these elements result from sensor malfunction, motor winding damage or inverter failure, among others; performance degradation and even safety risks are not ruled out. Such faults should be detected at an early stage to maintain the system's reliability and avoid unexpected breakdowns. Techniques of fault diagnosis are paramount to increase operation safety, reliability, and customer's trust on NEV technology. In particular, some hidden or potential faults of a battery system be detected by monitoring key electrical parameters (voltage, current) of the battery system. Efficient fault detection also enhances predictive maintenance strategies leading to less downtime and maintenance cost. As whole, it is essential for intelligent diagnosis methods to be designed to guarantee stability and high-efficiency in today's NEV systems.

1.1. Contribution

Using WT and FFT feature extraction, the Z-score-normalized voltage, current, motor speed, and ambient sensor data are inputted to ECS-AG-LSTM for precise and adaptive fault diagnosis of NEV.

The paper is structured as follows: Section 2 describes materials and methods including data preprocessing, FFT and WT feature extraction, and the proposed ECS-AG-LSTM model for NEV fault diagnosis; Section 3 presents experimental results and performance evaluation; and Section 4 concludes with key findings, limitations, and future research directions.

2. Materials and methods

ML and LSTM models effectively detect EV/NEV faults using sensor signals like current, voltage, and speed [7]. Data-driven ML-based FDD enhances EV safety by accurate battery and motor fault diagnosis and improvement of adaptiveness and predictive mitigation [8]. Hyperparameter-optimized neural network effectively classifies NEV motor drive bearing faults [9].

2.1. Methodology

NEV sensor data standardized using Z-score, FFT and WT extract features, ECS-AG-LSTM performs adaptive fault detection. interpolation and mean imputation preserved signal continuity and fault information. Fig. 1 shows the overall structure.

Data pre-processing using **Z** score normalization: Z-score normalization standardizes NEV sensor data for consistent fault diagnosis. Z-score normalization of NEV sensor signals improves gradient stability, feature quality, convergence, and fault classification performance. It is applied in Eq. (1):

$$W_{new} = \frac{\mathrm{W}-\mu}{\sigma} = \frac{W - \mathrm{Mean}(W)}{\mathrm{StdDev}(W)} \tag{1}$$

Feature extraction using FFT and WT: FFT and WT extract time-frequency features from NEV sensor data, improving transient fault detection accuracy. The FFT-WT hybrid method extracts frequency, time-frequency and non-stationary characteristics of the faults for precise NEV diagnosis.

FFT: The FFT converts NEV sensor signals from the time domain to the frequency domain, so that it identify the

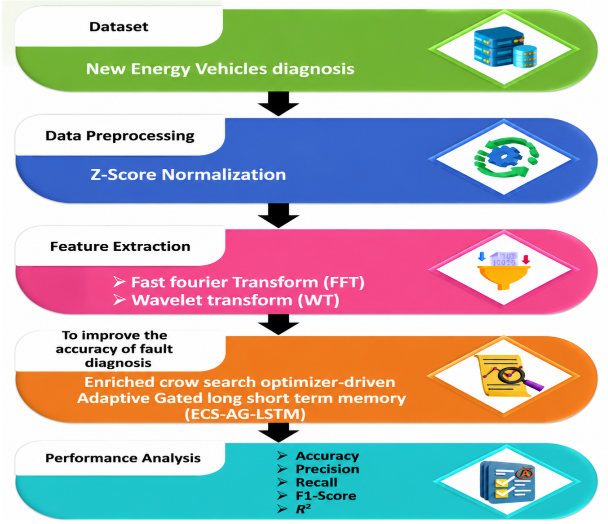

Fig. 1. NEV fault diagnosis framework workflow overview

unusual frequency patterns for good battery, inverter and motor fault diagnosis Eq. (2).

$$W(\zeta) = \int_{\infty}^{\infty} w(s) f^{-2\pi j \zeta s} ds \tag{2}$$

FFT enables fast computation compared to DFT. Here is a definition of the DFT in Eq. (3).

$$W_l = \sum_{m=0}^{M-1} w_m f^{-\frac{2wm}{M}}, (l = 0, .., M-1) \tag{3}$$

WT: WT allows adaptive time-scale analysis of NEV sensor signals for the identification of transient faults and hidden defects in all physical variable.

$$HFC_i = HFC_{i+1} g_1; LFC_i = LFC_{i+1} k_1, (i = 0, \dots, m-1) \tag{4}$$

$$HFC_i = HFC_{i+1} g_2 + LFC_{i+1} k_2, (i = m-1, \dots, 1, 0) \tag{5}$$

ECS-AG-LSTM: ECS-AG-LSTM combines optimization and gating for robust NEV fault detection. Algorithm 1 shows ECS-AG-LSTM.

ECS-AG-LSTM computational complexity considers efficiency, overhead, memory consumption, and the processing cost of AG-LSTM. For an input sequence length T, hidden neuron size H, and input feature dimension F, the computational complexity of AG-LSTM represented as $O\left(T \times \left(H^2 + HF\right)\right)$. Therefore, the optimization complexity of ECSA is expressed as $O(M \times NI \times \text{ Fitness })$.

2.1.1. *Integration of ECS and AG-LSTM for NEV Fault Diagnosis*

ECS with AG-LSTM performs parameter estimation by adaptive search, that is a good tradeoff between exploitation and exploration, result in better NEV fault diagnosis.

Algorithm 1. ECS-AG-LSTM for NEV Fault Diagnosis

Require: Training data $\mathcal{D}_{\text{train}}$
Ensure: Optimized ECS-AG-LSTM model
Initialize AG-LSTM
if pretrained weights are available **then**
  Load pretrained weights
else
  Initialize (W_g, b_g), (W_p, b_p), and (W, b) using Xavier initialization
Select GPU if available; otherwise select CPU
Initialize ECSA
Initialize a crow population of size M with random positions
for each iteration **do**
  for each crow **do**
    Update the position using adaptive probability based on memory or random movement
    Evaluate the fitness of the updated position
  Update crow memories and the global best solution
End-to-End Optimization
Optimize AG-LSTM weights using ECSA
Load the best optimized weights into AG-LSTM
Output the optimized ECS-AG-LSTM model

2.1.2. AG-LSTM

AG-LSTM merges gate, reduces complexity, improves NEV fault accuracy. Fig. 2 illustrates the structure of the AG-LSTM model. In the s^{th} period, forward propagation and equation of AG-LSTM are explained as follows.

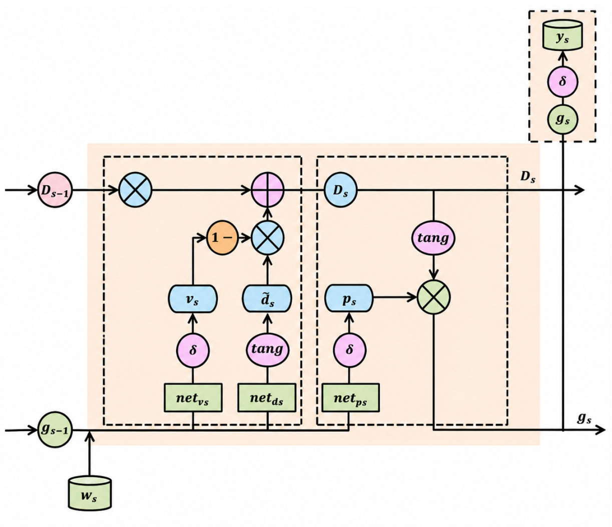

Fig. 2. Architecture of the Adaptive Gated Long Short-Term Memory (AG-LSTM) Unit

Determine the shared gates in Eq. (6) and Eq. (7) shows a neural network's net input calculation.

$$\text{net}_{vs} = X_v \cdot \begin{bmatrix} g_{s-1} \\ W_s \end{bmatrix} + a_v = X_{vg} \cdot g_{s-1} + X_{vw} \cdot w_s + a_v \tag{6}$$

$$v_s = \sigma\left(W_{vg} g_{s-1} + W_{vw} w_s + a_v\right) \tag{7}$$

$$\text{net}_{\tilde{d}s} = X_{\tilde{d}} \cdot \begin{bmatrix} g_{s-1} \\ W_s \end{bmatrix} + a_v = X_{\tilde{d}g} \cdot g_{s-1} + X_{\tilde{d}w} \cdot w_s + a_{\tilde{d}} \tag{8}$$

$$\tilde{d}_s = \tanh\left(\text{net}_{\tilde{d}}^{S}\right) \tag{9}$$

$$D_s = (1 - v_s) \odot D_{s-1} + v_s \odot \tilde{d}_s \tag{10}$$

$$net_{ps} = X_p \cdot \begin{bmatrix} g_{s-1} \\ W_s \end{bmatrix} + a_p = X_{pg} \cdot g_{s-1} + X_{pw} \cdot w_s + a_p \tag{11}$$

$$p_s = \sigma\left(net_{ps}\right) \tag{12}$$

$$g_s = p_s \odot \tanh\left(d_s\right) \tag{13}$$

$$y_s = X_z \cdot g_s + a_z \tag{14}$$

$$z_s = \sigma(ys) \tag{15}$$

$$\sigma(w) = \frac{1}{1 + e^{-w}}, \tanh(w) = \frac{e^{w} - e^{-w}}{e^{w} + e^{-w}} \tag{16}$$

AG-LSTM reduces LSTM gates, lowering parameters and training complexity. AG-LSTM ReLU improves stability, convergence, accuracy, robustness, temporal learning. Tanh processes state; update gate combines memory and input.

Crow Search Algorithm (CSA): ECS lacks clear novelty, as it does not demonstrate significant improvements, ablation studies. In the search space, the vector $w^{j,iter}$ indicates the location of the j th crow at time/iteration iter, where $i = 1, 2, \ldots, M$,iter $= 1, 2, \ldots$, iter max , and iter$_{\max}$.

ECS: ECSA enhances the optimization efficiency, the accuracy and the reliability of EV fault detection, as well as the safety of EVS. The ECSA achieves the balance of exploration and exploitation by adaptive parameter, memory update, and convergence-based optimization termination. The following is a description of the suggested ECSA and its primary steps

Stage 1: Initialize parameters. The ECSA parameters are established: awareness probability (AP), maximum number iterations (NI), the number of crows (M), decision variables (d).

Stage 2: Initialize the crows' initial location and memory. As the herd's members, start the M crows' positions in the search space at random. As follows, d is the number of choice variables, and every crow symbolizes a possible fix for the problem in Eq. (17):

$$w^{j,\text{iter}+1} = \begin{cases} w^{j,\text{iter}} + q \times EK^{j,\text{iter}} \times \left(m^{i,\text{iter}} - w^{j,\text{iter}} \right), & \text{if rand} > AP^{i,\text{iter}}, \\ \text{random position}, & \text{otherwise.} \end{cases} \tag{17}$$

$$\text{Crows} = \begin{bmatrix} w_1^1 & w_1^2 & \cdots & w_1^c \\ w_2^1 & w_2^2 & \cdots & w_2^c \\ \vdots & \vdots & \vdots & \vdots \\ w_M^1 & w_M^2 & \cdots & w_M^c \end{bmatrix} \tag{18}$$

It initializes each crow's memory; it is believed that have concealed their food in the following Eq. (19):

$$\text{Memory} = \begin{bmatrix} n_1^1 & n_1^2 & \cdots & n_1^c \\ n_2^1 & n_2^2 & \cdots & n_2^c \\ \vdots & \vdots & \vdots & \vdots \\ n_M^1 & n_M^2 & \cdots & n_M^c \end{bmatrix} \tag{19}$$

Stage 3: Assess the fitness function. The value of each crow's position is determined once the values of the chosen variable are entered into the target function.

Stage 4: Create a new role. Crow i is chosen at random to create a new position of the j th crow at the iteration i ter, and crow j, follows crow i, to find the hidden food. Every crow goes through this procedure once more, and Eq. (17) yields each crow's new location.

Stage 5: Analyze the feasibility of creating more positions. Each crow updates position if new location is viable. Otherwise, the population means (w^{mean}) and the global best position (w^{best}) is followed by the crow.

Stage 6: Assess the fitness function of newly created positions. For every new crow's position, the fit function value is calculated.

Stage 7: Updates to memory, thus, after the calculation, depending on the j th crow's storage is updated according to the position's fitness value, as shown in Eq. (20).

$$n^{j,\text{iter}+1} = \begin{cases} w^{j,\text{iter}}, & \text{if } e\left(w^{j,\text{iter}+1}\right) \text{ is better than } e\left(n^{i,\text{iter}+1}\right), \\ n^{i,\text{iter}}, & \text{otherwise.} \end{cases} \tag{20}$$

Stage 8: Assure the termination requirement with valid information. If iterations exceed NI, optimization terminates; stages 4-7 execute. ECSA improves AG-LSTM using adaptive search and convergence balance. The position mechanism of ECSA is mathematically expressed as:

$$w^{(j,iter+1)} = w^{(j,iter)} + q \times EK^{(j,iter)} \times \left(m^{(i,iter)} - w^{(j,iter)} \right) \tag{21}$$

Fault diagnosis

The parameters setup is: 3 LSTM gates, 64 neurons, ReLU, Softmax, Adam, 0.1 LR, 0.96 decay, 30 epochs, batch 64, 8 kernels, LR Scheduler. Hyperparameter tuning includes learning rate, batch size, epochs, hidden neurons, AP, crow population, decay, optimizer; ECS-AG-LSTM uses 70/15/15 split, 30 epochs, Softmax, and sparse categorical cross-entropy.

3. Results and discussion

3.1. Dataset

This work contains NEV sensor and fault data of motor, inverter, and battery diagnostics, which is useful for deep learning training and testing, with an 80/20 train-test ratio.

3.2. Performance metrics

The existing methods, including multi-level convolutional neural network, CNN [10], incipient bat-optimized deep residual network (IB-DRN) [11], MCNN [12], and LSTM [10], are evaluated in terms of recall, R^2, accuracy, precision, and F1-score. ECS-AG-LSTM software and hardware requirements include MATLAB R2024a as software, Intel i7 Core CPU as processor, 4 GB minimum RAM, Windows 11 (64-bit) operating system, ECS-AG-LSTM as the algorithm, and NEV diagnosis data as input. The confusion matrix measures the performance of ECS-AG-LSTM classification based on normal, inverter, battery and motor fault conditions, i.e., the number of correct and wrongly predicted samples.

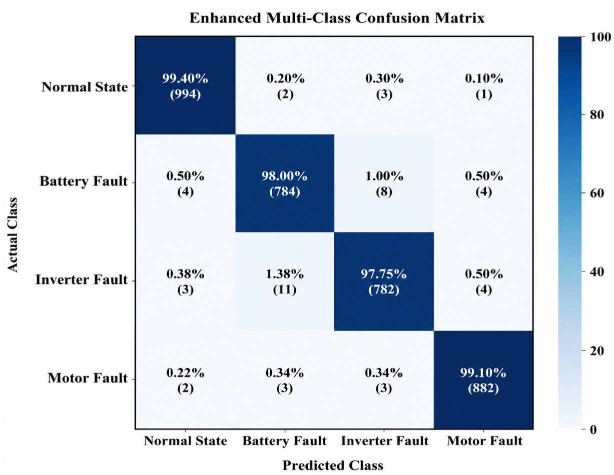

Fig. 3. ECS-AG-LSTM multi-class confusion matrix NEV fault diagnosis

ECS-AG-LSTM confusion matrix for normal, battery, inverter, and motor faults are shown in Fig. 3, and Table 1 verifies higher precision, recall, and F1-score.

Table 1. Class-wise Classification Performance of the Proposed ECS-AG-LSTM Model

Class	Precision (%)	Recall (%)	F1-Score (%)	Support
Normal State	99.20	99.40	99.30	1000
Battery Fault	98.20	98.00	98.10	800
Inverter Fault	97.90	97.80	97.85	800
Motor Fault	98.38	98.04	98.21	900
Macro Average	98.42	98.31	98.37	3500
Weighted Average	98.42	98.31	98.51	3500

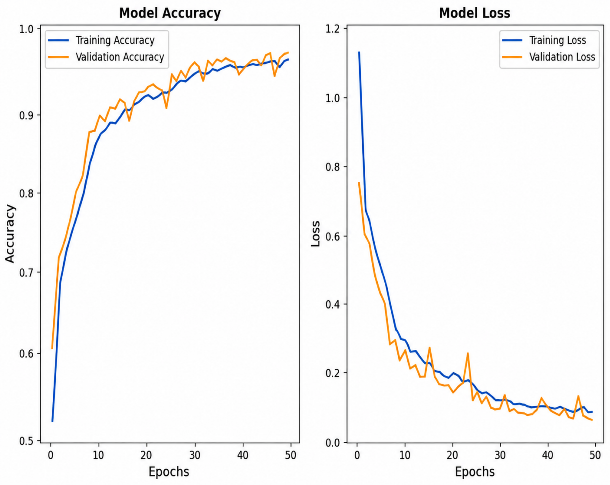

Fig. 4. Accuracy and loss for proposed ECS-AG-LSTM model

- Accuracy and loss: Fig. 4 shows the accuracy and loss of the proposed ECS-AG-LSTM model in NEV fault diagnosis.
- Accuracy: Fig. 5 shows the comparison of accuracy performance, the ECS-AG-LSTM achieves 98.5%, better than IB-DRN (98%) and MCNN (98.16%) in the NEV fault diagnosis.
- Precision: The suggested ECS-AG-LSTM method achieve 98.42% accuracy which are better than those of IB-DRN (90%) and MCNN (98.17%); Fig. 6 shows the comparison of accuracy results on the NEV fault diagnosis.
- Recall: The proposed ECS-AG-LSTM reaches a recall of 98.31%, surpassing IB-DRN (97%) and MCNN (98.16%); recall results NEV fault diagnosis are compared in Fig. 7.
- F1-score: The proposed ECS-AG-LSTM model achieves 98.51% F1-score, which is better than IB-DRN (94%) and MCNN (98.16%); Fig. 8 present comparisons of F1-score for NEV fault diagnosis.

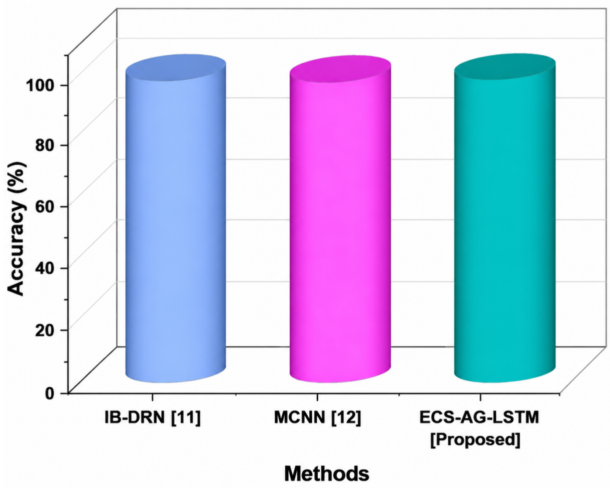

Fig. 5. Accuracy performance of proposed and existing strategies

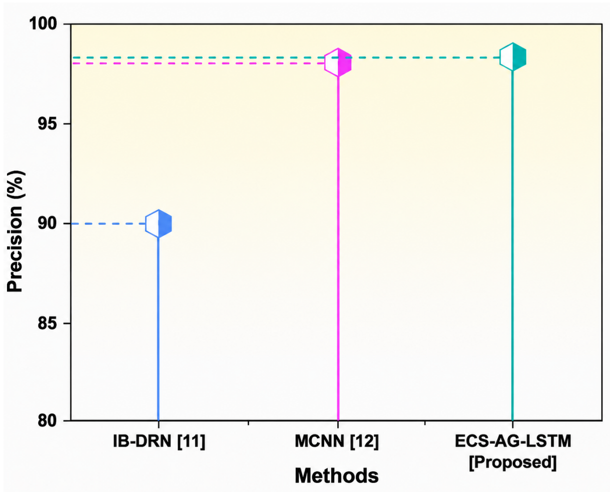

Fig. 6. Comparison result of Precision for proposed and conventional strategies

- R^2 : The suggested ECS-AG-LSTM has an R^2 value of 0.956 , is better than CNN (0.874) and LSTM (0.935); R^2 performances for NEV fault detection are compared.

IB-DRN [11] achieves 98% accuracy, 90% precision, 97% recall, and 94% F1-score; MCNN [12] achieves 98.16% accu-

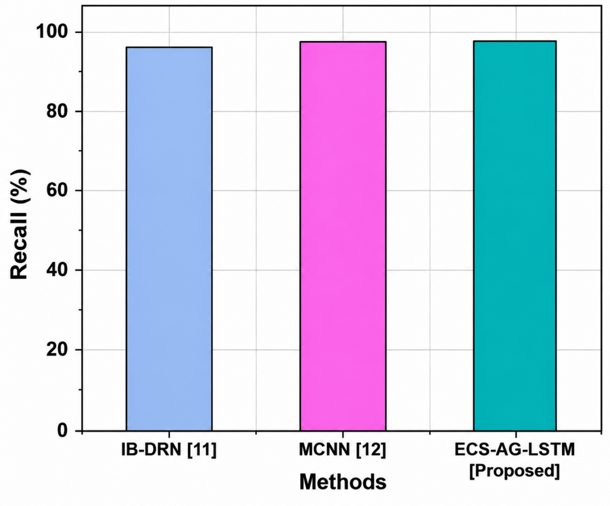

Fig. 7. Visual representation of proposed and existing methods

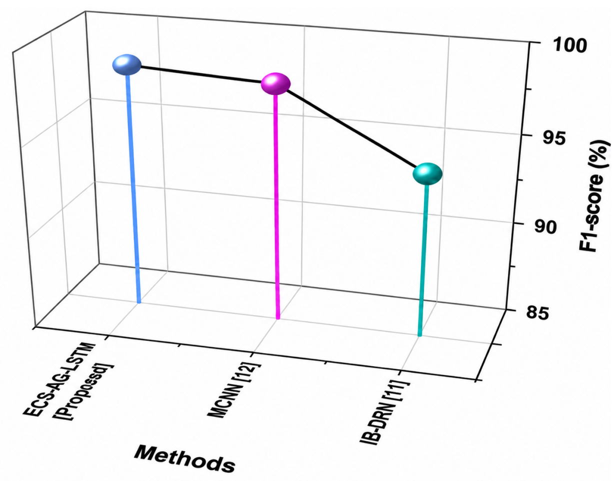

Fig. 8. F1 score performance of proposed ECS-AG-LSTM and existing strategies

racy, 98.1% precision, 98.16% recall, and 98.16% F1-score; and the proposed ECS-AG-LSTM achieves 98.5% accuracy, 98.42% precision, 98.31% recall, and 98.51% F1-score. CNN [10] achieves R^2 value of 0.874 , LSTM [10] achieves 0.935 , and the proposed ECS-AG-LSTM achieves 0.956, showing superior performance. ECS-AG-LSTM enables real-time NEV fault diagnosis using BMS (3.0-4.2 V, 300-800 V, 0-300 A, -20 °C-65°C), motor data (0-6000 rpm, 0-400 Nm, 0-250 A), vibration (0-10 kHz), and CAN (250 kbps-1 Mbps), achieving 98.5% accuracy, 98.42% precision, 98.31% recall, 98.51% F1-score, and 0.956R^2, outperforming MCNN, CNN, IBO-DRN, and LSTM.

3.3. Feature Importance Analysis of Extracted NEV Signals

Feature importance analysis of voltage, temperature, vibration, wavelet, FFT features, and motor speed shows normalized values enable accurate NEV fault classification; vibration (0.21), FFT features (0.19), wavelet coefficients (0.18), voltage (0.16), motor speed (0.14), and temperature (0.12).

3.4. Error Analysis and Misclassification Study of ECS-AG-LSTM Model

Error analysis of ECS-AG-LSTM shows Normal Operation (245 TP, 3 FP, 5 FN, 3.15% misclassification), Inverter Fault (238 TP, 6 FP, 7 FN, 5.16%), Battery Fault (240 TP, 4 FP, 6 FN, 4.00%), Motor Fault (236 TP, 8 FP, 10 FN, 7.03%), and Sensor Fault (242 TP, 5 FP, 4 FN, 3.61%).

3.5. Ablation Study of ECS-AG-LSTM Model for Component-wise Performance Evaluation

The contributions of ECS, AG-LSTM, WT and FFT are evaluated in ablation study; the full model achieves the best performance, as summarized in Table 2 fault diagnosis performance.

3.6. Fault Severity Prediction Analysis for Predictive Maintenance in NEV Systems

Fault severity prediction categorizes NEV faults by employing multiple features, with ECS-AG-LSTM reaching 97.8% battery, 98.1% inverter, 98.6% motor, 97.5% sensor, and 98.3% thermal fault accuracy associated with risk and maintenance levels.

3.7. Energy Efficiency and Computational Sustainability Analysis

Energy assessment confirms a lower consumption of ECS-AG-LSTM (1.65 kWh, 4.3 mJ/sample, 55% CPU, 310 MB, low overhead) compared with CNN, LSTM, MCNN, and IBO-DRN.

3.8. Convergence Analysis with Learning Rate Scheduling

Learning rate scheduling improves ECS-AG-LSTM performance by increasing accuracy from 94.1% to 97.8%, reducing epochs from 48 to 29, lowering loss from 0.092 to 0.041, improving stability from moderate to high, changing convergence from slow oscillatory to fast smooth, reducing oscillation from high to low, and increasing generalization from 0.89 to 0.96.

Table 2. Ablation Study of the ECS-AG-LSTM Model for NEV Fault Diagnosis

Model Variant	ECS	AG-LSTM	WT	FFT	Accuracy (%)	Precision (%)	Recall (%)	F1-Score (%)
Without ECS	×	✓	✓	✓	96.20	96.10	96.00	96.15
Without AG-LSTM	✓	×	✓	✓	95.10	95.05	94.90	95.00
Without WT	✓	✓	×	✓	94.60	94.50	94.40	94.45
Without FFT	✓	✓	✓	×	95.00	94.85	94.70	94.78
Full Model	✓	✓	✓	✓	98.50	98.42	98.31	98.51

3.9. Generalization Capability and Robustness Analysis

K-fold cross-validation tests the stability of the generalization of ECS-AG-LSTM among folds; the results in Fig. 9 demonstrate robustness of the estimation.

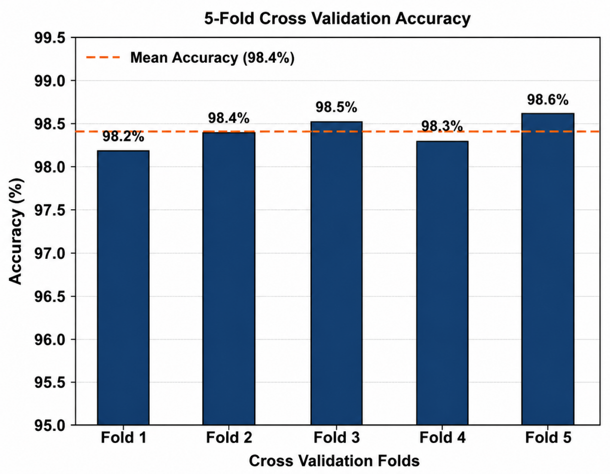

Fig. 9. K-Fold Validation Accuracy of ECS-AG-LSTM

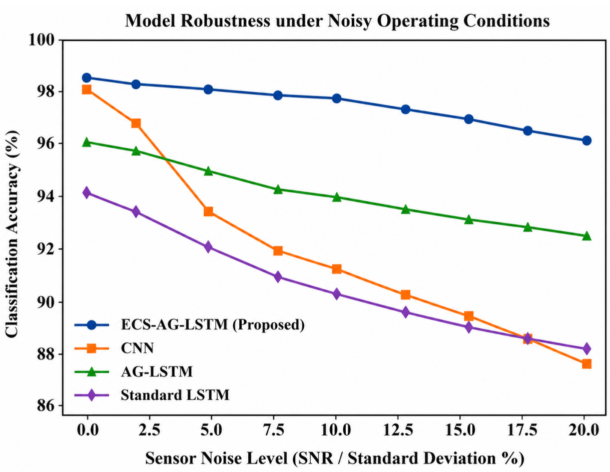

Fig. 10. Robustness of ECS-AG-LSTM and baselines under increasing sensor noise levels

Fig. 10 shows ECS-AG-LSTM robustness (98.5%, 97.9%, 97.5%, 97.2%, 97.4%, 96.8%) outperforming AG-LSTM, LSTM, and CNN across all noise conditions.

3.10. Training Dynamics and Convergence Analysis

The learning stability and accuracy and loss curves of ECS-AG-LSTM are analysed; Fig. 11 indicates that the optimization is stable and the performance is good.

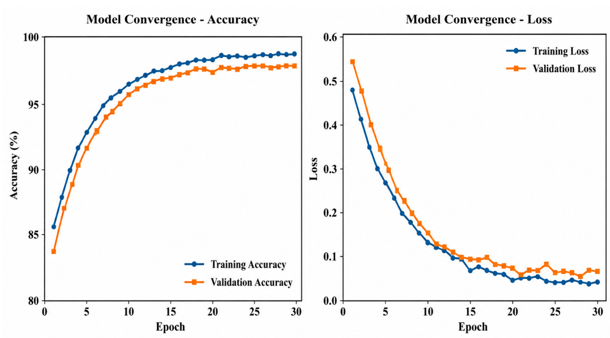

Fig. 11. ECS-AG-LSTM learning curves show convergence behavior

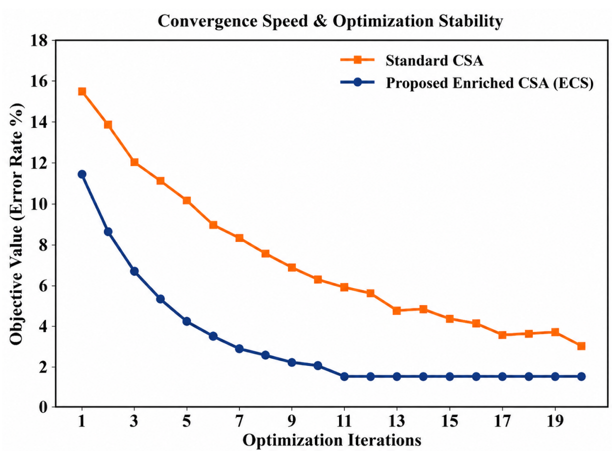

Fig. 12. ECS shows faster convergence greater optimization stability than standard CSA

As shown in Fig. 12, ECS converges more rapidly and stably than CSA with lower objective values; computational efficiency comparison shows CNN (1,245,616 parameters, 210 s training, 0.42 ms inference), Standard LSTM (452,380 parameters, 340 s training, 0.85 ms inference), AG-LSTM (321,240 parameters, 240 s training, 0.58 ms inference), and ECS-AG-LSTM (321,240 parameters, 265 s training, 0.58 ms inference, 1240 s optimization*).

3.11. External Validation and Generalization Capability Analysis

ECS-AG-LSTM shows strong generalization and cross-domain robustness. It obtains 98.5% accuracy on NEV Drivetrain Dataset (industrial/private, 17,500 samples) with good generalization, 97.8% on Kaggle NEV Dataset (12,000 samples) with very good results, 97.3% on CWRU Bearing Dataset (8,500 samples) with strong cross-domain ability, and 96.9% on NASA Li-ion Battery Dataset (6,000 samples).

4. Discussion

Analysis of the NEV fault in IB-DRN, MCNN, CNN, and LSTM is less feasible due to high computation, data requirements, overfitting, and black-box characteristic [11]. CNN is computationally expensive and requires a large amount of labeled data [10], whereas MCNN is incompetent when dealing with noisy and unbalanced data [12]. The ECS-AG-LSTM is extended to the HEV and FCEV, with enhanced FFT, WT, and adaptive learning for better fault diagnosis. Robust models improve accuracy and generalization using FFT and WT. Transfer learning improves ECS-AG-LSTM generalization and reduces retraining cost. Diagnostic techniques and fault-tolerant control for electric vehicle powertrain are intensively investigated to enhance the reliability and running safety of EV systems under diverse conditions [13]. Such methods emphasize the need for resilient diagnostics that can detect and compensate for faults in critical drivetrain elements including motors and power electronics. The application of bearing fault diagnosis for SSM using multisenor data fusion proves that KINS algorithm has good performance in enhancing detection accuracy of faults in electric vehicle powertrains [14].

5. Conclusion

In NEV systems, fault diagnosis entails analyzing sensor data to identify and categorize issues with vital parts like the battery, inverter, and motor. By employing ECS-AG-LSTM techniques to detect and categorize drivetrain system issues, this research attempted to create an advanced fault detection system for NEVs. The dataset, which includes operating and malfunction data as well as sensor data including voltage, current, motor speed, and temperature, is intended for use in diagnosing drivetrain problems in NEVs. Z score normalization was used to pre-process the data, while FFT and WT were used to extract the features. The method achieves better performance contrasted to the existing approaches in terms of accuracy (98.5%), recall (98.31%), R^2(0.956), precision (98.42%), and F1 score (98.51%). It consists of the fact that models cannot be easily applied to different kinds of operations and the necessity to use clean labeled data.

6. Limitations and future research

The ECS-AG-LSTM architecture, especially when optimized by ECSO, is computationally intensive. This makes real-time or edge deployment challenging without significant hardware resources. Develop lightweight versions of the ECS-AG-LSTM model for real-time inference and integration into onboard diagnostic systems of NEVs.

7. Acknowledgement

Author thanks Hunan Mechanical & Electrical Polytechnic, Changsha, China, for academic environment and technical support enabling completion of this research work.

8. Declaration

Data Availability: https://www.kaggle.com/datasets/ziya07/fault-diagnosis-dataset-for-new-energy-vehicles/data

Conflicts of Interest: The author declares no conflicts of interest regarding the publication of this paper.

Funding Statement: No external funding received.

Author Contribution: Zhengqian Wu solely contributed to the conception, design, data collection, analysis, and writing of this manuscript.

Ethical Approval: This study involves no human, so ethical approval was not required.

Consent to Participate: Not applicable.

Consent to Publication: The author consents to the publication of this manuscript.

Competing Interests: The author declares there are no competing interests related to this work.

References

[1] Y. Chen, J. Zhang, S. Zhai, and Z. Hu, (2024) *"Data-Driven Modeling and Fault Diagnosis for Fuel Cell Vehicles Using Deep Learning"* **Energy AI *16***: 100345. DOI: 10.1016/j.egyai.2024.100345.

[2] C. S. A. Gong, C. H. S. Su, and K. H. Tseng, (2020) *"Implementation of Machine Learning for Fault Classification on Vehicle Power Transmission System"* **IEEE Sensors Journal *20***(24): 15163–15176. DOI: 10.1109/JSEN.2020.3010291.

[3] H. Kaplan, K. Tehrani, and M. Jamshidi, (2021) *"A Fault Diagnosis Design Based on Deep Learning Approach for Electric Vehicle Applications"* **Energies** ***14***(20): 6599. DOI: 10.3390/en14206599.

[4] M. U. I. Khan, M. I. H. Pathan, M. M. Rahman, M. M. Islam, M. A. R. Chowdhury, M. S. Anower, et al., (2024) *"Securing Electric Vehicle Performance: Machine Learning-Driven Fault Detection and Classification"* **IEEE Access**: DOI: 10.1109/ACCESS.2024.3400913.

[5] M. Z. Khaneghah, M. Alzayed, and H. Chaoui, (2023) *"Fault Detection and Diagnosis of the Electric Motor Drive and Battery System of Electric Vehicles"* **Machines** ***11***(7): 713. DOI: 10.3390/machines11070713.

[6] X. Liang, P. Wang, X. Cao, X. Wan, P. Chao, X. Zhao, et al., (2025) *"Research on Improving the Safety of New Energy Vehicles Exploits Vehicle Operating Data"* **Safety Science** ***181***: 106681. DOI: 10.1016/j.ssci.2024.106681.

[7] H. Liu, X. Song, and F. Zhang, (2021) *"Fault Diagnosis of New Energy Vehicles Based on Improved Machine Learning"* **Soft Computing** ***25***(18): 12091–12106. DOI: 10.1007/s00500-021-05860-9.

[8] P. Wang, J. Chen, F. Lan, Y. Li, and Y. Feng, (2024) *"Multiscale Feature Fusion Approach to Early Fault Diagnosis in EV Power Battery Using Operational Data"* **Journal of Energy Storage** ***98***: 112812. DOI: 10.1016/j.est.2024.112812.

[9] Y. Wang and W. Li, (2021) *"Transfer-Based Deep Neural Network for Fault Diagnosis of New Energy Vehicles"* **Frontiers in Energy Research** ***9***: 796528. DOI: 10.3389/fenrg.2021.796528.

[10] Y. Zhang, C. Liao, M. Liu, and Z. She, (2024) *"PLC Technology Under the New Energy Vehicle Motor Drive System Fault Detection Research"* **Journal of Electrical Systems** ***20***(9s): 537–545.

[11] J. Zhao, X. Feng, J. Wang, Y. Lian, M. Ouyang, and A. F. Burke, (2023) *"Battery Fault Diagnosis and Failure Prognosis for Electric Vehicles Using Spatiotemporal Transformer Networks"* **Applied Energy** ***352***: 121949. DOI: 10.1016/j.apenergy.2023.121949.

[12] K. Zhao and H. Bai, (2024) *"Safety Management System of New Energy Vehicle Power Battery Based on Improved LSTM"* **Energy Informatics** ***7***(1): 101. DOI: 10.1186/s42162-024-00411-6.

[13] C. Wu, R. Sehab, A. Akrad, and C. Morel, (2022) *"Fault Diagnosis Methods and Fault Tolerant Control Strategies for the Electric Vehicle Powertrains"* **Energies** ***15***(13): 4840. DOI: 10.3390/en15134840.

[14] X. Wang, S. Lu, K. Chen, Q. Wang, and S. Zhang, (2021) *"Bearing Fault Diagnosis of Switched Reluctance Motor in Electric Vehicle Powertrain via Multisensor Data Fusion"* **IEEE Transactions on Industrial Informatics** ***18***(4): 2452–2464. DOI: 10.1109/TII.2021.3095086.